Materials Today Communications 36 (2023) 106478

Contents lists available at ScienceDirect

Materials Today Communications

journal homepage: www.elsevier.com/locate/mtcomm

Fabrication, structural, thermo-mechanical and opto-electrical behavior of anthranilamide compound

S. Dinagaran [a], J. Gajendiran [b,*], S. Gokul Raj [c,*], S. Gnanam [d], J. Ramana Ramya [e], S.Rafi Ahamed [f], C. Esther Jeyanthi [g]

[a] Department of Physics, University College of Engineering Thirukkuvalai, Thirukkuvalai 610204, Tamilnadu, India
[b] Department of Physics, Vel Tech Rangarajan Dr.Sagunthala R&D Institute of Science and Technology, Avadi, Chennai 600 062, India
[c] Department of Physics, C.Kandaswami Naidu College for Men, Annanagar, Chennai 600102 Tamilnadu, India
[d] Department of Physics, School of Basic Sciences, Vels Institute of Science, Technology & Advanced Studies (VISTAS), Pallavaram, Chennai 600 117, India
[e] Department of Periodontics, Saveetha Dental College and Hospitals, Saveetha Institute of Medical and Technical Sciences (SIMATS), Chennai 600077, India
[f] Department of physics, Academy of Maritime Education and Training (AMET), Kanathur, Chennai 603112, India
[g] Department of Physics, Panimalar Engineering College, Chennai-600 123, India

ARTICLE INFO

Keywords:
Structural characteristics
Optical properties
Thermal behavior
Mechanical properties
Electrical properties

ABSTRACT

Anthranilamide (AAM) compound were fabricated via an alcoholic solvent assisted slow evaporation at room temperature for investigating the multi functional device applications. The solubility test was performed with different concentrations of AAM salt dispersed in 100 mL ethanol solvent to understand the crystallization process of fabricated material. The cell parameters, and diffraction peaks of the title compound were collected through nondestructive tool like single crystal XRD and powder XRD studies, and thus results showed the monoclinic structure. The fabricated material's functional group, thermal stability, and hardness behavior were tested by various tool viz FT-IR, TG-DTA, and Vickers hardness analysis. With the aid of UV–vis–NIR spectrum, and frequency conversion test technique, optical transmittance and double harmonic generation efficiency values are detected to be 92% and 4.1 mV. Using electrical studies, the dielectric parameters and specific conductance of the title compound values are varied by applying a low frequency to a high frequency region at different temperatures (313, 323, and 333 K).

1. Introduction

Nonlinear optical crystals that are inorganic, semi-organic, and organic have a wide range of utilization in information technology, optoelectronics, light transmission storage devices, frequency conversion, and mixing etc. [1–8]. Especially, organic material exhibits much higher frequency conversion efficiencies, and faster response in opto-electric based switches than their inorganic material, and thus leads to applicable for light sensing devices [7,8]. In this present work, the optical transmittance spectrum, mechanical hardness test, and electrical study revealed that synthesized AAM material have a 92% optical transmittance in the visible light, acceptable optical transmission quality and stability, moderate hardness, low dielectric loss, and conductivity. The above-mentioned feature of the title compound can be used in multifunctional device applications. Jin et al. [9], Hergett et al. [10], Hu et al. [11], Mythili et al. [12], and Liang et al. [13] used solution growth, slow evaporation, optical floating zone method, microwave plasma chemical vapor deposition, Czochralski pulling technique, and melt growth assisted single crystal to tested the NLO and electro-optics related device applications. The slow evaporation route is chosen for the following reasons: low operating temperature, without using any instruments or tedious process applying pressure and high temperature [7,8].

In the current work, AAM are fabricated from ethanol solvent assisted slow evaporation technique followed by characterized various instruments like single crystal XRD, powder XRD, FT-IR, UV, SHG, thermal, mechanical and electrical analysis. The above-mentioned title compound characterization outcomes are explained in elaborated. The synthesized AAM material exhibits good transmittances in the visible region, as confirmed by the UV spectrum analysis. According to electrical studies, dielectric loss, dielectric constant, and AC conductivity values are tuned depending on the applied frequency and a set of

* Corresponding authors.
E-mail addresses: gaja.nanotech@gmail.com (J. Gajendiran), sgokulraj@gmail.com (S.G. Raj).

https://doi.org/10.1016/j.mtcomm.2023.106478
Received 2 May 2023; Received in revised form 12 June 2023; Accepted 17 June 2023
Available online 19 June 2023

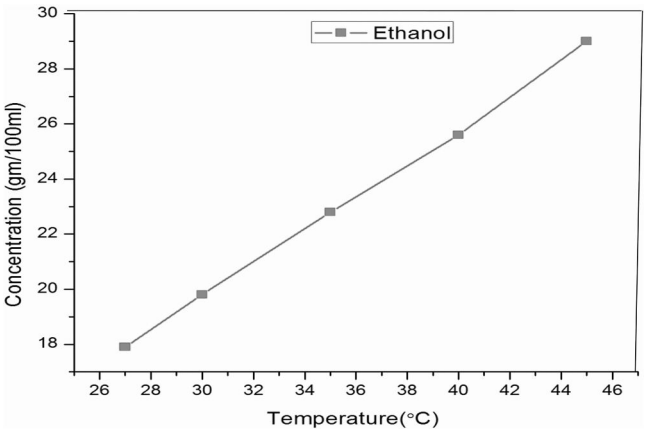

Fig. 1. Solubility test of AAM salt concentration dispersed in 100 mL ethanol at temperature of 26–46 °C.

Table 1
Crystallographic data of AAM material.

Unit cell parameters	Obtained values from the single crystal XRD
a	14.05 Å
b	6.31 Å
c	7.83 Å
α	90°
β	97.67°
γ	90°
V	687 Å^3

different temperatures. The above -mentioned properties are suitable for electro-optic device applications. The synthesized AAM material has been tested by Kurtz and Perry powder route with solid-state laser (Nd: YAG) for investigation frequency conversion applications.

2. Experimental

Anthranilamide (AAM) compound were developed through mixing of anthranilamide salt with an ethanol solvent followed by slow solvent evaporation technique. The commercially available anthranilamide solid was cleaned with ethanol by several times repeating crystallization process, consequently it was taken as a purified precursor for fabricate of the title compound. 100 mL ethanol solvent was preserved in a beaker and a certain amount of purified precursor was gradually added under magnetic stirred continuous processing temperature from 26° to 46°C to reach the supersaturated solution. The supersaturated solution was filtered in a petty disc followed by preserved it for 10 days in order to fabricate the AAM material. The AAM material was taken and it's characterized the cell parameters, optical transmittance, frequency conversion efficiency, thermal and material stability, and electrical properties. The above said features can be used to identify various tools like single crystal XRD, powder XRD, FT-IR, TGA, UV–visible, NLO, mechanical and electrical instruments (Supporting Information).

Solubility test was performed with various concentration of anthranilamide dispersed in 100 mL of ethanol solvent under magnetic stirring at temperatures between 26 and 46 °C, as displayed in Fig. 1. The supersaturated solution was obtained, 29 g of anthranilamide dispersed in 100 mL of ethanol solvent, temperature processed at 45 °C.

3. Results and discussion

The six parameters of unit cell (length of each side (a, b, c), interfacial angles (α, β,γ)), as well as the cell volume of the fabricated compound can be collected using single crystal XRD analysis, and the obtained values are mentioned in Table 1. Further, collections of unit

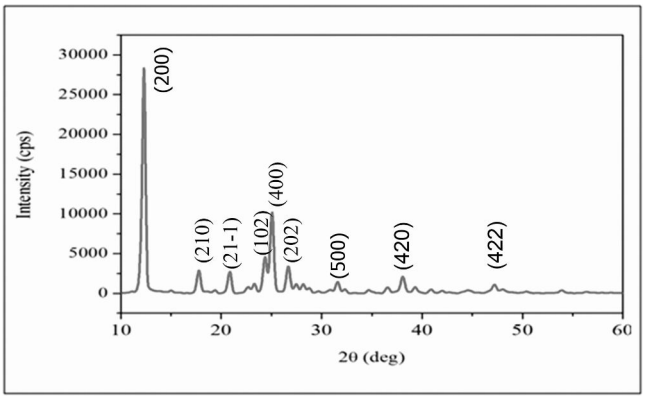

Fig. 2. Powder XRD spectrum of AAM material.

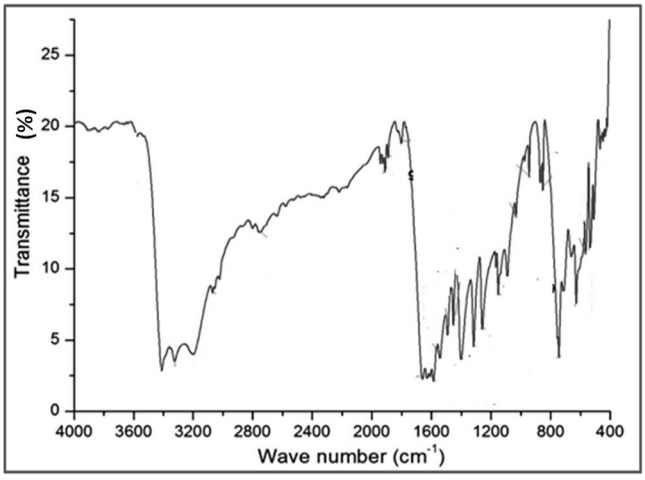

Fig. 3. FT-IR spectrum of AAM material.

Table 2
The detected bands wave number and its corresponding vibrational band assignments of AAM material.

Wave number (cm^{-1})	Vibration Assignments
3839	OH stretching
3411	OH stretching
3324	NH_2 stretching
3199	NH_2 stretching
3069	C-H stretching
1659	C═O stretching
1401	C═C stretching
1316	C-N stretching
1257	C-N stretching
943	C-H out of plane bending

cell parameters from Table 1 reveals that the synthesized AAM material has respect to formation of a monoclinic crystal system with the space group $P2_1/c$ (ICDD code No.00–004–0435).

The presence of a few strong intensity sharp peaks in the obtained XRD pattern of the title compound (Fig. 2) shows the material's good crystalline behavior [12]. In addition, the observed diffraction peaks of 12.70°, 18.96°, 21.27°, 24.60°, 25.50°, 27.75°, 32.11°, 38.47°, and 47.11° corresponding planes are indexed in the XRD pattern as (200), (210), (21−1), (102), (400), (202), (500), (420), and (422), respectively.

The chemically attached functional groups of the AAM material are recorded with the assed of FT-IR spectrum, and are shown in Fig. 3. The recorded FT-IR vibrational band assignment of the synthesized AAM

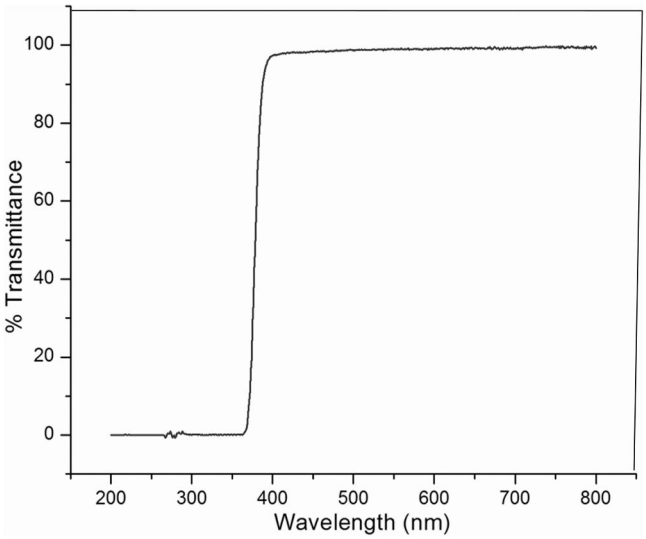

Fig. 4. UV-Vis transmittance spectrum of AAM material.

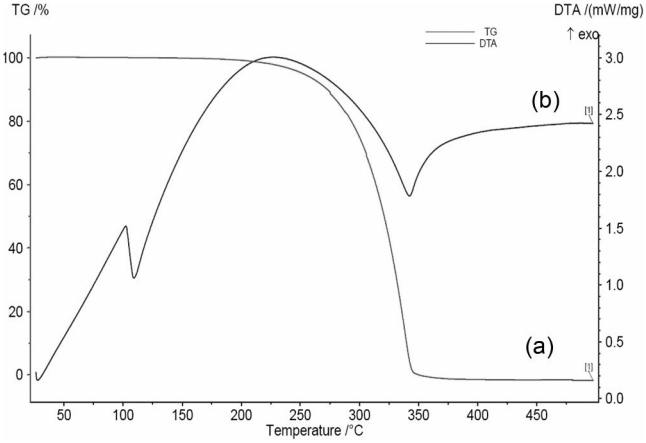

Fig. 5. TGA-DTA curve of AAM material.

material is carefully noticed and consolidated in Table 2. The recorded vibrational bands of the fabricated compound are checked to the reported vibrational frequency and functional groups of the anthranilamide [14]. The obtained FT-IR results indicate that the synthesized compound is anthranilamide.

Kurtz and Perry powder route with solid state laser (Nd:YAG), beam energy 1.1 mJ/pulse, pulse width 8 ns with repetition frequency rate 10 Hz was operated to identify the SHG efficiency value of the synthesized AAM material. The SHG value of the synthesized AAM material is determined to be 4.1 mV, which compares to the standard crystals SHG values of KDP (4 mV) and Urea (34 mV). The synthesized AAM material exhibits centrosymmetric behavior; however, the SHG value is approximately 1.03 times that of KDP. Due to the presence of defects, internal stress, or surface effects in the synthesized material [15–17].

The transmittance quality of the synthesized AAM material was evaluated via UV-Vis-NIR transmittance spectrum with wavelength ranging from 200 to 800 nm (Fig. 4). According to Fig. 4, the cut off wavelength in the UV region is around 364 nm. The above mentioned optical transmittances of the synthesized compound reveal that it has a good transparency of ~ 92% after reaching a wavelength of 390 nm in the UV region. The synthesized AAM material exhibits good transmittance in the visible region. This behavior in the visible region is suitable for frequency conversion based device applications [18,19].

TGA/DTA study was introduced to test the ability of the synthesized AAM material to withstand certain temperatures, as shown in Fig. 5a. There is an utmost weight loss of the fabricated material in the temperature range from 260 °C to 340 °C. The weight loss mentioned above indicates residue removal from the fabricated material. The first endothermic peak at 112 °C on the DTA curve (Fig. 5b) indicates the starting point for the material's decomposition, confirming that the material can retain its texture until 112 °C. Another endothermic broad peak obtained at 355 °C demonstrates the compound's volatile substance liberation.

Vickers hardness tests were used to examine the material behavior (softness or hardness) of the AAM material, and the results are discussed in this section. In this study, a diamond indenter was pressed against the plane of synthesized AAM material with a load ranging from 25 to 100 g, and the resulting indentation was determined. For all trials, the indentation time interval was set to 25 s. The hardness (H_v) values are changes observed as a result of the processing load P, as displayed in Fig. 6a. According to the graph above, hardness values increase with increasing load, satisfying the normal indentation effect [8].

The material hardness or softness determined by Vickers hardness analysis is dependent on the work hardening coefficient (n). The n value ranges from 1 to 1.6, with larger than 1.6 denoting stiffness and soft material nature behavior, respectively. A plot of log P versus log d (Fig. 6b) yields a straight line and the slope of the line gives the Meyer's indexes, which are 3.07 according to the Meyer's relation. Hence, based on the n value results represent that fabricated AAM material are of a moderately soft material. The obtained moderately soft behavior reveals that the crystalline defect in the synthesized AAM

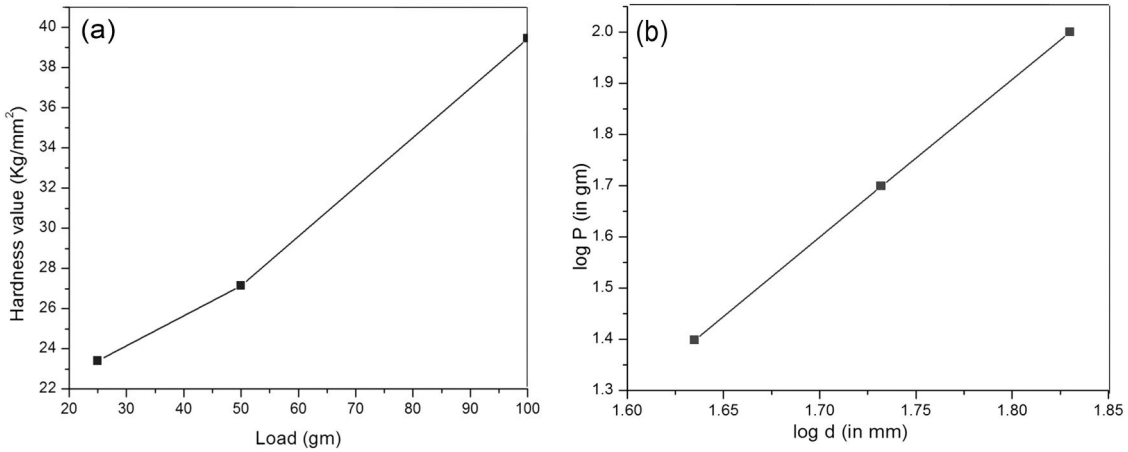

Fig. 6. (a) Plot of Vicker's hardness versus load P, and (b) log P versus log d of the AAM material.

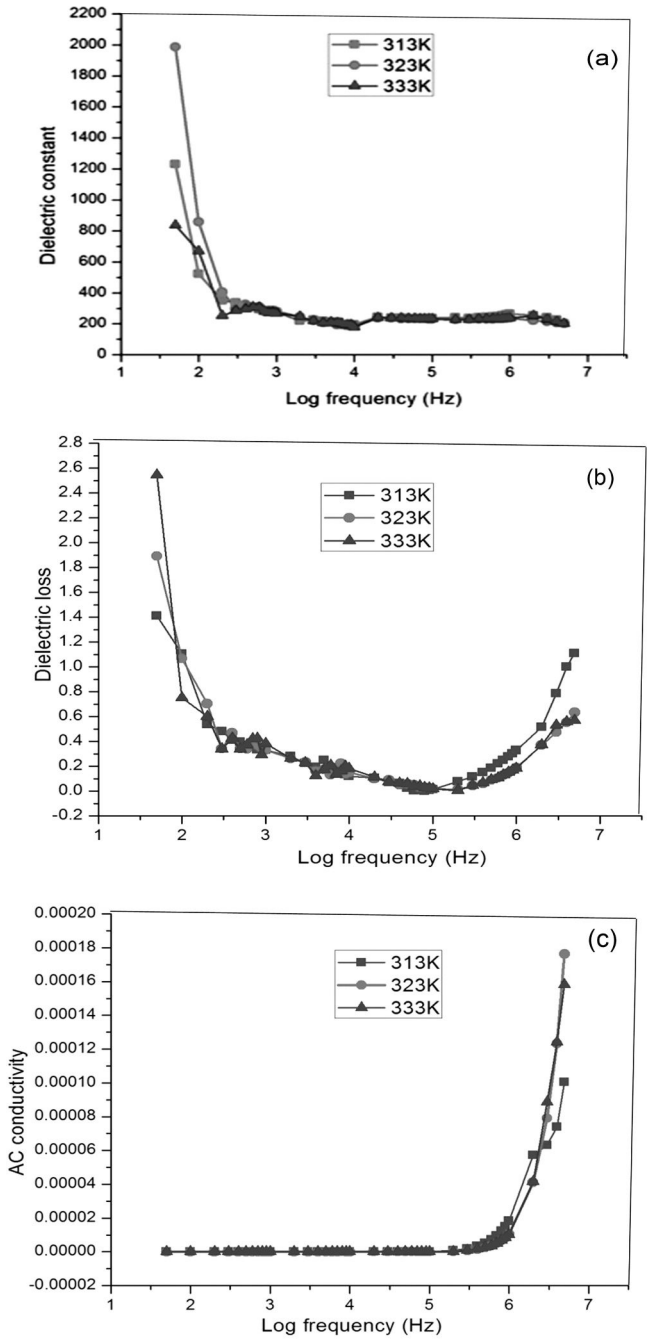

Fig. 7. a. Dielectric constant vs. logarithmic frequency of the fabricated AAM material.b. Dielectric loss vs. logarithmic frequency of the fabricated AAM material.**c.** Electrical conductivity vs. logarithmic frequency of the fabricated AAM material.

material.

The dielectric properties of solid materials vary depending on the applied electric field distribution. The relative dielectric constant and dielectric loss of a material can be providing about the blocking or movement of charge carrier activity. Fig. 7a shows how dielectric constants change when changing from a lesser frequency to a higher frequency region for all temperatures (313, 323, and 333 K). The dielectric constant decreases with increase in frequency (1.5–2.48 Hz) and remains constant at higher frequencies portion (i.e. from 2.48 to 6.75 Hz). Further, all four types of polarization (electronic, ionic, orientation, and space charge) are present in the fabricated material, which explains why dielectric constant values are higher in the low frequency region [20–25]. The dielectric constant was high at low frequencies. This is because space charge polarization exists at the grain boundaries, creating a potential barrier. The charge then accumulated at the grain boundary, resulting in higher values of the real part of permittivity. According to Miller's rule, a lower dielectric constant at higher frequency is a preferable for increasing SHG efficiency [26].

Frequency on the X-axis, and dielectric loss on the Y-axis were plotted for the synthesized AAM material and its results are presented in Fig. 7b. For all temperatures (313, 323 and 333 K), the four types of polarization mechanisms mentioned above contribute to a higher value of the dielectric constant in the lesser frequency region. The samples' has found low dielectric loss at high frequency region in the electrical studies [27]. The synthesized AAM material has improved optical transmission ability with less deformity. The above said characteristics are applicable for the frequency conversion devices.

Fig. 7c depicts the AC conductivity vs. frequency of the AAM material at three different temperatures (313, 323, and 333 K). The nearly uniform value of AC conductivity at frequencies ranging from 1.5 to 5.98 Hz is inferred from Fig. 7c. This was due to the blocking of electron or ion hopping in the low frequency portion. For all temperatures, AC conductivity values increase above 6 Hz. This was caused by hopping electrons or ions in the higher frequency portion. AC conductivity values are relatively higher at temperature set of 333 K than at other temperatures set (313 and 323 K) as presented in Fig. 7c. According to electrical studies, AC conductivity values are tuned depending on the applied frequency and a set of different temperatures.

4. Conclusion

Anthranilamide compound were synthesized through an alcoholic solvent slow evaporation technique. The AAM material belongs to the monoclinic system, according to the single crystal XRD and powder XRD analyses. Using optical transmittance spectrum analysis of the synthesized AAM material, optical transmittance has found to be constant in the visible region. Vibrational bands and thermal stability of the AAM material were examined with the FT-IR and TGA/DTA analysis. The title compound's SHG efficiency value is found to be relatively greater than that of the standard reference KDP crystal. The results of the micro hardness tests show that the AAM material has a moderate strength. The results of the optical, NLO, and electrical characterization imply that the anthranilamide compound could be a viable for the fabrication of electro-optics and nonlinear optical devices.

CRediT authorship contribution statement

S. Dinagaran: Methodology, Investigation, Writing – original draft. **J. Gajendiran:** Investigation, Writing – original draft, Writing – review & editing, Conceptualization. **S. Gokul Raj:** Investigation, Writing – original draft, Writing – review & editing. **S. Gnanam:** Investigation, Writing – original draft, Writing – review & editing. **J. Ramana Ramya:** Writing – review & editing. **S Rafi Ahamed:** Formal analysis. **C. Esther Jeyanthi:** Formal analysis.

Declaration of Competing Interest

The authors declare the following financial interests/personal relationships which may be considered as potential competing interests: S. Gokul Raj reports a relationship with C Kandaswami Naidu College for Men that includes: funding grants. S. Dinagaran reports a relationship with University College of Engineering Thirukkuvalai that includes: non-financial support.

Data availability

Data will be made available on request.

Appendix A. Supporting information

Supplementary data associated with this article can be found in the online version at doi:10.1016/j.mtcomm.2023.106478.

References

[1] S. Kavitha, R. Ezhil Vizhi, J. Mol. Struct. 1276 (2023), 134746.
[2] Muhammad Rashid, Junaid Yaqoob, Nida Khalil, Rashida Jamil, Muhammad Usman Khan, Mazhar Amjad Gilani, Mater. Sci. Semicond. Process. 151 (2022), 107007.
[3] D. Wang, X. Meng, N. Zhang, D. Sun, R. Hou, H. Chen, X. Liu, Opt. Mater. 135 (2023), 113225.
[4] K. Bouchouit, Z. Essaidi, S. Abed, A. Migalska-Zalas, B. Derkowska, N. Benali-cherif, M. Mihaly, A. Meghea, B. Sahraoui, Chem. Phys. Lett. 455 (2008) 270–274.
[5] Rumyana Yankova, Ivaylo Tankov, Tanya Tsaneva, J. Mol. Struct. 1273 (2023), 134307.
[6] V. Chithambaram, S. Jerome Das, S. Krishnan, J. Alloy. Compd. 509 (2011) 4543–4546.
[7] P. Lalitha, S. Arumugam, A. Sinthiya, C. Nivetha, M. Muthuselvam, Results Chem. 5 (2023), 100790.
[8] K. Savitha, K. Saravanan, J. Cryst. Growth 582 (2022), 126529.
[9] W. Jin, L. Gai, C. Li, H. Lin, L. Su, A. F.Zeng, Wu, Phys. B Condens. Matter 588 (2020), 412168.
[10] W. Hergett, C. Neef, H. Wadepohl, H.P. Meyer, M.M. Abdel-Hafiez, C. Ritter, E. Thauer, R. Klingeler, J. Cryst. Growth 515 (2019) 37–43.
[11] W. Hu, K. Chen, T. Tao, X. Yu, J. Zhou, Z. Xie, B. Liu, R. Zhang, Thin Solid Films 763 (2022), 139571.
[12] A. Mythili, K. Srinivasan, J. Cryst. Growth 601 (2023), 126946.
[13] W. Liang, L. Zhang, X. Xiang, J. Wang, L. Zhang, B. Wu, Y. Wang, Y. Zeng, S. Guan, Q. Tang, F. Peng, Solid State Commun. 327 (2021), 114206.
[14] S. Thabet, B. Ayed, A. Haddad, Comptes Rendus Chim. 18 (2015) 979–985.
[15] M. Shakir, S.K. Kushwaha, K.K. Maurya, Manju Arora, G. Bhagavannarayana, J. Cryst. Growth 311 (2009) 3871–3875.
[16] A.M. Petrosyan, J. Cryst. Growth 311 (2009) 2484–2489.
[17] K. Muthu, Subbiah Meenakshisundaram, J. Cryst. Growth 352 (2012) 163–166.
[18] S. Natarajan, S.A. Martin Britto, E. Ramachandran, Cryst. Growth Des. 6 (2006) 137–140.
[19] N. Vijayan, R. Ramesh Babu, R. Gopalakrishnan, P. Ramasamy, J. Cryst. Growth 267 (2004) 646–653.
[20] J.S. Pan, X.W. Zhang, Acta Mater. 54 (2006) 1343–1348.
[21] T. Suthan, N.P. Rajesh, P.V. Dhanaraj, C.K. Mahadevan, Spectrochim. Acta Part A Mol. Biomol. Spectrosc. 75 (2010) 69–73.
[22] T. Suthan, N.P. Rajesh, J. Cryst. Growth 312 (2010) 3156–3160.
[23] T. Suthan, P.V. Dhanaraj, N.P. Rajesh, C.K. Mahadevan, G. Bhagavanarayana, Cryst. Eng. Comm. 13 (2011) 4018–4024.
[24] S. Prince, T. Suthan, C. Gnanasambandam, J. Electron. Mater. 51 (2022) 1639–1652.
[25] M.L. Lima Rose, T. Suthan, C. Gnanasambandam, T.C. Sabari, Girisun, J. Mater. Sci. Mater. Electron. 34 (2023) 884.
[26] U. Von Hundelshausen, Phys. Lett. A 34 (1971) 405–406.
[27] C. Balarew, R. Dehlew, J. Solid State Chem. 55 (1984) 1–6.